

1 The IceTop Scintillator Upgrade

The IceCube-Gen2 Collaboration[†]

[†] http://icecube.wisc.edu/collaboration/authors/icrc17_gen2

E-mail: samridha.kunwar@desy.de

The IceCube Neutrino Observatory at the South Pole probes the high-energy cosmic-ray sky by investigating the muonic and electromagnetic component of air showers measured with IceTop and the in-ice detector. However, more detailed measurements are needed to understand the astrophysics of the high-energy cosmic-ray sky. This, along with the need to mitigate the impact of snow accumulation on IceTop tanks, has given us impetus for further upgrades including scintillator and SiPM-readout-based stations. Prototype stations showcasing technological advances for the next generation in cosmic ray detection are currently under construction for deployment at South Pole in December 2017. We describe the physics and the current status of the project.

Corresponding authors: Thomas Huber^{1,3}, John Kelley², Samridha Kunwar^{*3}, Delia Tosi²

¹ *Institut für Kernphysik, Karlsruhe Institute of Technology, D-76021 Karlsruhe, Germany*

² *Dept. of Physics and Wisconsin IceCube Particle Astrophysics Center, University of Wisconsin, Madison, WI 53706, USA*

³ *DESY, D-15738 Zeuthen, Germany*

*35th International Cosmic Ray Conference — ICRC2017
10–20 July, 2017
Bexco, Busan, Korea*

*Speaker.

1. Introduction

IceCube is a cubic-kilometer neutrino detector installed in the ice at the geographic South Pole [1] between depths of 1450 m and 2450 m, which was completed in 2010. Reconstruction of the direction, energy, and flavor of the neutrinos relies on the optical detection of Cherenkov radiation emitted by charged particles produced in the interactions of neutrinos in the surrounding ice or the nearby bedrock. Additionally, an array of surface detectors, IceTop, has also been deployed for cosmic ray studies in the PeV energy range [2] and to provide a partial veto of the down-going background of penetrating muons.

Accumulating snow cover of the IceTop tanks is continuously increasing the energy threshold for the detection of cosmic ray air showers [3]. The complex attenuation effects of the snow add systematic uncertainties to air shower measurements, particularly in the mass composition analysis. We have designed and proposed an upgrade to IceTop consisting of an homogeneously-spaced scintillator array with an areal coverage similar to IceTop. Currently we plan on deploying up to 37 scintillator stations over several years as shown in Fig 1. Each scintillator station comprises of seven scintillator panels communicating with a central hub as shown in Fig 2.

This upgrade is planned for two phases of deployment. Phase 1, marked in red in Fig. 1, will enable us to study the effect of attenuation on high-energy air showers. As stations are added during phase 2, marked in green in Fig. 1, the coverage will improve and the energy sensitivity will expand to include low-energy air showers.

2. System Overview

We are exploring different detector designs as prototype solutions for the upgrade. The system (Fig. 2) features the following building blocks:

- The scintillator panel subsystem. Extruded plastic scintillators are used in combination with wavelength-shifting fibers to collect and guide the light produced by an energetic particle crossing the scintillator. The fibers are read out by one light sensor. The detector is enclosed in a mechanical structure, designed to be light-tight and provide protection from harsh environmental conditions.

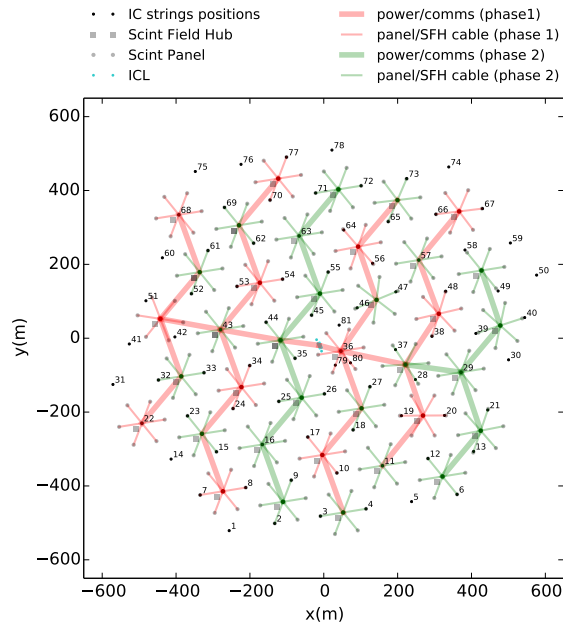


Figure 1: Map of the scintillator array as designed for the IceTop upgrade, in IceCube coordinates. Each number denotes the location of an existing IceTop station.

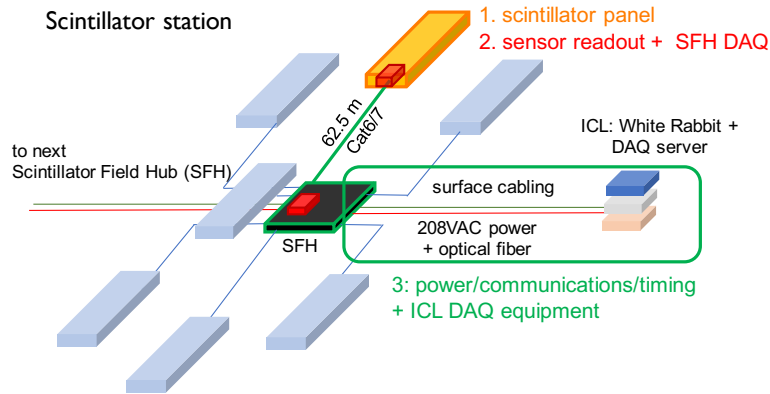


Figure 2: Scintillator station with 7 scintillator panels connected to a Field Hub DAQ featuring White Rabbit timing. The three building blocks as described in the text are highlighted.

- 40 • The DAQ subsystem: the light sensor is read out and data are processed by a custom-designed
- 41 data acquisition system.
- 42 • The Scintillator Field Hub (SFH) subsystem includes data handling, power, and timing dis-
- 43 tribution between the IceCube Laboratory (ICL) and each scintillator station. It also includes
- 44 equipment in the ICL.

45 We have developed multiple realizations for each of the building blocks to explore different

46 solutions in terms of costs and complexity. In the following sections we describe each subsystem

47 in more detail.

48 **3. The scintillator panel subsystem**

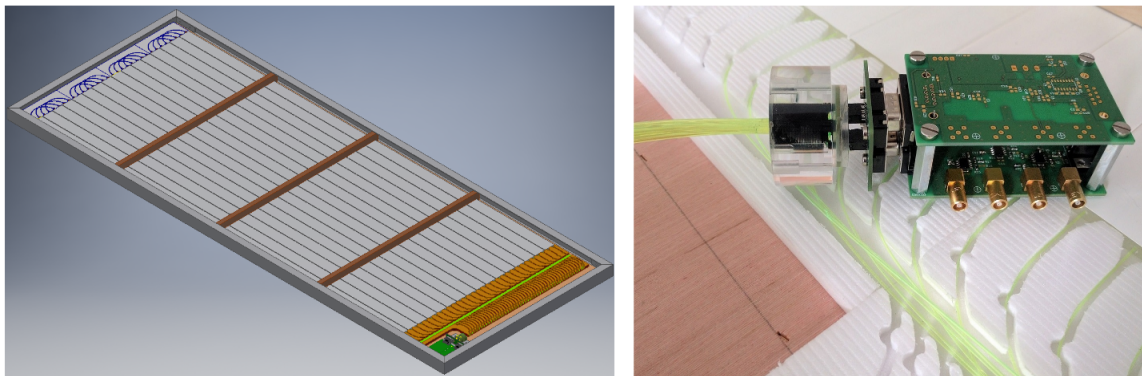


Figure 3: Left: Layout of the detector without top plate. The detector is placed in an aluminum frame to provide support. Right: optical fiber routing, plastic scintillator bars and a prototype of the Analog Readout Module for the IceTAXI Design (sec. 4.1), fully attached to the optical coupling of the detector. The SiPM is inside the cookie coupler which connects the optical fibers with the cookie board.

49 The detector design utilizes the low-cost customizable geometry of extruded scintillators sim-

50 ilar to those adopted by many other particle physics experiments in recent decades, such as SciBar

51 at K2K [4], the T2K near detector [5], MINERvA [6], and Auger Prime [7].

52 The unit detector is designed to have a total sensitive area of 1.5 m^2 and a total weight of less
53 than 50 kg, to be easily transportable by two people. Each panel comprises 16 extruded plastic
54 scintillator bars (produced on the FNAL/NICADD¹ Extrusion Line), made of polystyrene with
55 doping of 1% PPO and 0.03% POPOP and coated with a $0.25 \text{ mm} \pm 0.13 \text{ mm}$ thick layer of TiO_2
56 reflector. Each bar is 1 cm thick, 5 cm wide and 1.875 m long and has two holes with a diameter of
57 $2.5 \pm 0.2 \text{ mm}$. Two Y-11(300) wavelength shifter fibers (produced by Kuraray²) are routed into the
58 two holes of two bars, resulting in a bundle of 32 fiber ends which is then readout by a $6 \times 6 \text{ mm}^2$
59 Silicon PhotoMultiplier (SiPM).

60 We are currently exploring the use of either 0.7 mm or 1 mm fiber, which offer different ad-
61 vantages in terms of cost and light yield. The light yield has been studied with a detailed GEANT4
62 [8] simulation of the apparatus, resulting in 82.3 ± 23.9 and 137.1 ± 36.7 photons absorbed in the
63 SiPM for the 0.7 mm and 1 mm fiber respectively.

64 The fiber routing inherits features that were intensively studied for the AugerPrime upgrade of
65 the Pierre Auger Observatory with the goal of optimizing sensitivity and uniformity. The bars are
66 wrapped in opaque Velostat (ESD) material to ensure light-tightness. An outer aluminum shell and
67 an aluminum frame provide support. A prototype panel is shown in Fig. 3.

68 Two types of coupling are being explored. In the first type, the bundled fibers are cast into
69 a solid cookie with the fiber ends being cut and heated on a hot glass plate ensuring robustness
70 and long term stability. The cookie is then glued into a PMMA (Polymethyl methacrylate) coupler
71 along with the SiPM on a PCB — the cookie board. A 1 mm gap between the SiPM and the
72 fiber ends is filled with optical glue (EJ-500³) suited for low temperatures. This gap allows the
73 illumination of every pixel on the SiPM and thereby increases the dynamic range. The second
74 coupling makes use of a custom designed printed circuit board (PCB) that features holes of the
75 same diameter as the fiber and are homogeneously spaced to guarantee illumination of the whole
76 sensor active area. The fibers are threaded into the PCB and glued with a cold-rated epoxy. The
77 bundle is then cut and polished with a slant cabochon lapidary polisher. The fiber bundle is then
78 pressed against the SiPM surface with a spring loaded mechanism, with or without coupling gel.

79 4. The DAQ subsystem

80 4.1 IceTAXI

81 In this design, the SiPM is first connected to an analog readout module that comprises: the
82 cookie board with analog and digital temperature sensors; an adapter board designed for mechani-
83 cal stability that allows the cookie board and SiPM to be mounted inside the cookie; a readout board
84 that houses the power supply for the SiPM and three different pre-amplifiers ($\times 1$, $\times 5$, $\times 10$); and
85 finally, a general purpose board that contains line drivers to transmit the analog signal from the
86 scintillator panel to the SFH and a micro-controller for slow control (temperature, current, and
87 voltage monitoring and control) via an RS485 connection.

¹<http://www.fnal.gov/facilities>

²<http://kuraraypsf.jp>

³<http://www.ggg-tech.co.jp/maker/eljen/ej-500.html>

88 The IceTAXI DAQ is an
 89 FPGA + ARM embedded Linux
 90 system as shown in Fig. 4.1
 91 that was developed for the TAXI
 92 board supports 24 analog input
 93 channels in three blocks of eight
 94 channels each. A slightly modi-
 95 fied version of the board, IceTAXI,
 96 with one block of eight channels
 97 was produced for the IceTop scin-
 98 tillator array. Each channel is discriminated and the leading and trailing edges of the discriminator
 99 output are timestamped in a Spartan 6 FPGA with nanosecond precision. To achieve this, the output
 100 from the individual discriminators are interfaced with Serial-Input Parallel-Output (SIPO) Serial-
 101 izer Deserializer (SerDes) blocks in the FPGA with a 8:1 ratio at 950MHz. The subsequent 8-bit
 102 parallel output is then recorded at 118.75 MHz. In addition, input waveforms are recorded with a
 103 switched capacitor array and the integrated charge is determined online in the FPGA. The pulse
 104 time information and the charge-integrated or full waveform are then transferred to an ARM mi-
 105 crocontroller unit running Linux that handles the data formatting and transmission to the IceCube
 106 Laboratory via a 1 Gb fiber link under a White Rabbit layer.
 107

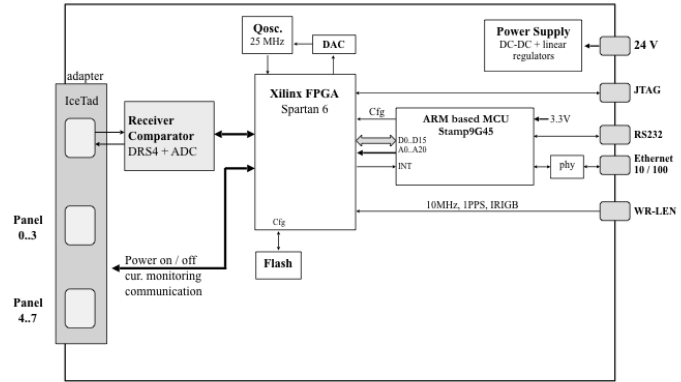


Figure 4: Layout of the IceTAXI Board.

4.2 μ DAQ

108
 109 The μ DAQ is a small microprocessor-
 110 based DAQ board (Fig. 4.2) dedi-
 111 cated to a single sensor (SiPM
 112 connected to a scintillator panel)
 113 that includes power, timing and
 114 communications hub and spokes
 115 for medium remote connection
 116 (~ 60 m). The microprocessor,
 117 along with inexpensive logic, cap-
 118 tures sensor pulse start and stop
 119 with ~ 1 ns resolution. To achieve
 120 this, eight delayed inputs are used
 121 such that each input sees the same
 122 edge delayed by successive ~ 1 ns increments before being recorded into “counter capture” regis-
 123 ters that increment every 5.5 ns (180 MHz). Averaging multiple delayed inputs results in higher
 124 time resolution. The board also features amplifiers, with multiple gains for a wide dynamic range,
 125 after which the pulse is shaped for sample-and-hold ADCs from which charge is obtained versus
 126 time.

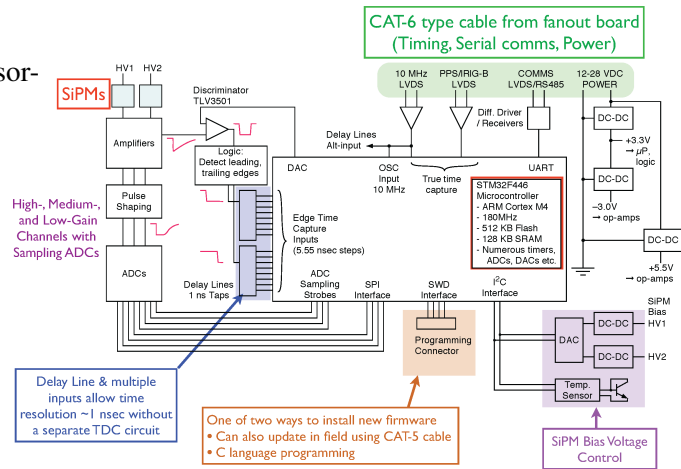


Figure 5: Layout of the μ DAQ Board

127 The μ DAQ design enables digitizing the signal at the output of the SiPM before transmission
 128 to the SFH. At the SFH, a Linux single-board computer (Beagle Bone Black) polls the seven panels,
 129 each with their own μ DAQ, and then forwards data to the IceCube Laboratory over optical fiber.

130 5. The Scintillator Field Hub subsystem

131 Communications, power, and timing for the scintillator array is accomplished via a network
 132 of Scintillator Field Hubs connected to backbone surface cabling to the IceCube Laboratory (ICL).
 133 Each SFH is the central DAQ node for a scintillator station (Fig. 2). The SFHs are synchronized
 134 to better than nanosecond precision by a White Rabbit (WR) Ethernet network [10], where the
 135 timing reference is a GPS receiver, and each SFH contains a WR node connected via single-mode
 136 optical fiber to a WR switch in the ICL. This link also provides gigabit Ethernet connectivity to
 137 each Scintillator Field Hub. The WR node in the SFH (WR-LEN⁴) provides timing and Ethernet
 138 connectivity to the DAQ via a copper Ethernet connection and two timing outputs: a reference 10
 139 MHz clock, and a 1-PPS IRIG-B timestring. A separate copper cable supplies the power to each
 140 SFH.

141 6. Prototype detector efficiency in a Muon Tower

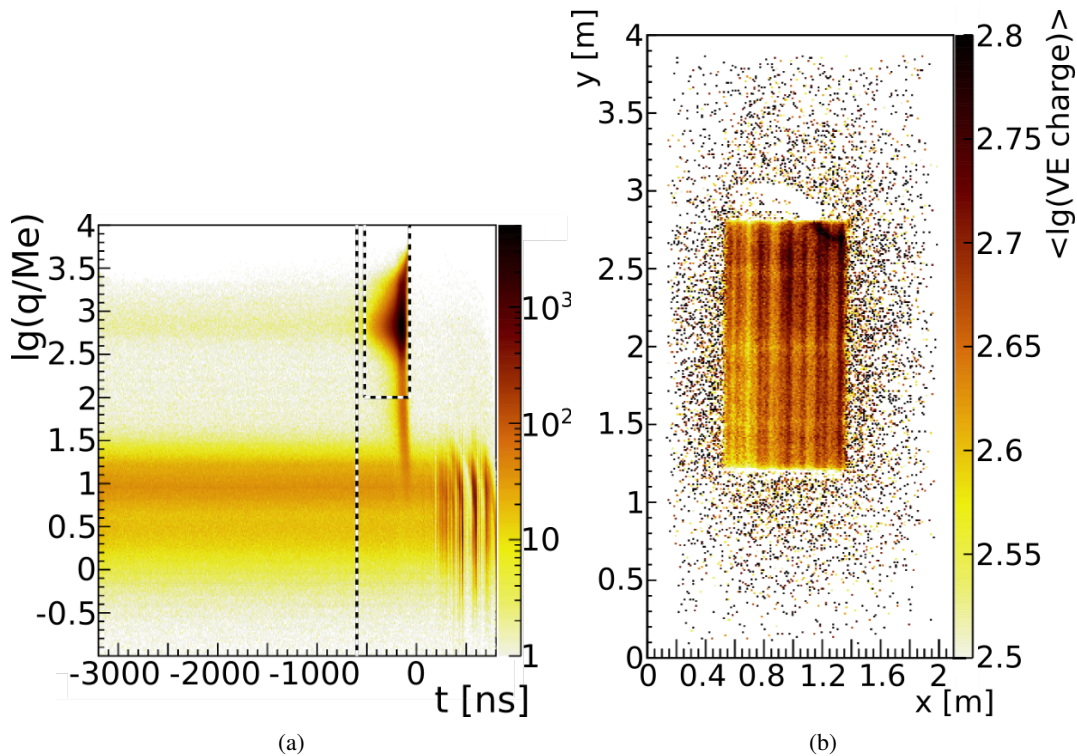


Figure 6: Left: Charge and time distribution of pulses detected with the prototype detector. The top region shows the high-charge band. The lower region the low-charge band and hence the SPE and the baseline. The dashed rectangle shows the quality cut for the MIPs. The distance between the high and low charge band shows the high light yield of a MIP compared to the base line. Right: Average pulse charge depending on the particle detection position. Single fibers are visible. Broken fibers or scintillators can be located and replaced. The higher average pulse charge located at $x=1.2$ m $y=2.8$ m arises because the fiber bundle coupled to the analog readout module, was for prototyping purposes just placed at the surface of the scintillator bars.

⁴<http://sevensols.com/index.php/products/wr-len/>

142 The Karlsruhe Institute of Technology (KIT) Muon Tower is a muon tracking detector with
143 limited streamer tubes (LST) originally from the KASCADE experiment and presently used for
144 calibration and efficiency measurements of scintillation detectors. The muon tower is capable of
145 tracking muons with an angular resolution of better than 1° and providing accurate position of
146 muons for the test detectors. This enables obtaining single photoelectrons (SPEs) and the amount
147 of SPEs per minimum ionizing particles (MIPs) in the test detector via a charge spectrum. Ad-
148 ditionally, muon tomography is also possible. Due to the LST, the Muon Tower has an in-plane
149 resolution of 1 cm^2 that allows for correction of the zenith angle when calculating the average
150 charge for vertical MIPs. It is also possible to investigate the efficiency and uniformity of the
151 inner detector system (scintillator bars, routing of optical fibers, optical connection). The charge
152 spectrum for through-going muons is shown in Fig. 6, left.

153 The plot in Fig. 6 (right) shows the average pulse charge depending on the particle position in
154 a logarithmic scale. Due to the optimal positioning of the fibers to the photosensitive surface of the
155 SiPM, the routing of the single fibers is visible. Due to this tomography-like feature of the muon
156 tower, broken scintillators or fibers can be located and replaced.

157 7. Summary & Outlook

158 We are currently developing a scintillator-based prototype detector as an upgrade to IceTop.
159 Each detector comprises 7 panels based on scintillator bars read out with wavelength shifting fibers
160 coupled to the photosensitive area of the SiPMs. We are investigating different options for fiber
161 diameter and fiber-to-sensor coupling.

162 Currently, two versions of DAQs are being explored; one featuring an embedded system ca-
163 pable of capturing full waveforms and the other comprising a small microprocessor with timing
164 and waveform capture with digital transmission of the data to the Beagle Bone Black based Field
165 Hub. White Rabbit provides timing and communications to the individual detectors. We anticipate
166 deploying a pair of prototype detectors in the 2017/18 Antarctic summer with an eventual phased
167 deployment of an array of up to 37 stations planned in the future.

168 References

- 169 [1] IceCube Collaboration, M. G. Aartsen et al., *J. Inst.* **12** (2017) P03012.
170 [2] IceCube Collaboration, R. Abbasi et al., *Nucl. Instr. Meth. A* **700** (2013) 188 – 220.
171 [3] IceCube Collaboration, M. .G. Aartsen et al., *POS (ICRC2015)* **628** (2015).
172 [4] K. Nitta et al., *Nucl. Instr. Meth. A* **535** (2004) 147.
173 [5] F. Retière et al. (T2K Collaboration), TIPP 2011 proceedings, *Phys. Proc.* **37** (2012) 1231 – 1240.
174 [6] MINERvA Collaboration, K. S. McFarland et al., *Nucl. Phys. Proc. Suppl.* **159** (2006) 107 .
175 [7] Pierre Auger Collaboration, A. Aab et al., arXiv:1604.03637 (2016).
176 [8] E. Dietz-Laursonn et al., *J. Inst.* **12** (2017) 4P04026.
177 [9] T. Karg, A. Haungs, M. Kleifges et al., arXiv:1410.4685 (2014).
178 [10] P.P.M. Jansweijer, H.Z. Peek, and E. de Wolf, *Nucl. Instr. Meth. A* **725** (2013) 187 – 190.